Kinetics of the Reaction of CH_3O_2 + NO: A Temperature and Pressure Dependence Study with Chemical Ionization Mass Spectrometry

Asan Bacak, Max W. Bardwell, M. Teresa Raventos,‡ Carl J. Percival,*,‡ Gabriela Sanchez-Reyna,† and Dudley E. Shallcross†

The School of Science, The Nottingham Trent University, Clifton Lane, Nottingham, NG11 8NS, United Kingdom, and Biogeochemistry Research Centre, School of Chemistry, University of Bristol, Cantock's Close, Bristol, BS8 1TS, UK

Received: May 24, 2004; In Final Form: September 20, 2004

The overall rate coefficient (k_4) for the reaction CH_3O_2 + NO → products (4) has been measured by using the turbulent flow technique with chemical ionization mass spectrometry (CIMS) for the detection of reactants and products. The temperature dependence of the rate coefficient was investigated between 193 and 300 K. Across the temperature range the experimentally determined rate coefficients were fitted by using an Arrhenius type analysis to yield the expression $k_4 = (1.75^{+0.28}_{-0.24}) \times 10^{-12}$ exp[(435 ± 35)/T] cm^3 molecule^{-1} s^{-1}. Experiments were carried out at 100 and 200 Torr total pressure within the stated temperature range, where the rate coefficients were shown to be invariant with pressure. The branching ratio of the reaction was also assessed as a function of temperature and was found to proceed 100 ± 10% via the channel forming CH_3O + NO_2, there being no discernible increase in the yield of CH_3ONO_2 at low temperatures. This work represents the first study of the branching ratio as a function of temperature and pressure. Previous studies have shown that the rate coefficient displays a negative temperature dependence, with the suggestion that the reaction rate increases with increasing pressure as well as increasing with decreasing temperature. This study lends weight to the assertion that there is no pressure effect (in agreement with a recent theoretical study) and that differences between previous studies at low temperature are most likely to be experimental errors. A model of the troposphere has been used to assess the impact of the experimental error of the rate coefficients determined in this study on predicted concentrations of a number of key species, including O_3, OH, HO_2, NO, and NO_2. In all cases it is found that the propagated error is very small and will not in itself be a major cause of uncertainty in modelled concentrations. However, at low temperatures where there is a wide discrepancy between existing kinetic studies, modelling using the range of kinetic data in the literature shows a relatively large variation for CH_3O_2, HCHO, and minor reservoir species such as HO_2NO_2 and $CH_3O_2NO_2$. Such a discrepancy may have implications for observationally driven models operating in regions of the troposphere below 240 K.

Introduction

Methane is the most abundant organic compound present in the earth's atmosphere. Natural sources of methane include anaerobic bacterial fermentation in water containing organic waste such as natural wetland areas and oceans and intestinal fermentation in wild animals. Anthropogenic sources of methane include intestinal fermentation in cattle, sewer gas, and combustion sources.[1] In the daytime troposphere the dominant sink for methane is by hydrogen abstraction upon reaction with the hydroxyl radical, shown in reaction 1.

$$CH_4 + OH \rightarrow CH_3 + H_2O \quad (1)$$

$$CH_3 + O_2 + M \rightarrow CH_3O_2 + M \quad (2)$$

$$CH_3O_2 + HO_2 \rightarrow CH_3OOH + O_2 \quad (3)$$

The alkyl radical produced in reaction 1 then reacts exclusively with oxygen to form the methylperoxy radical, reaction 2. In the clean troposphere the main fate of the methylperoxy radical is by reaction with the hydroperoxy radical as shown in reaction 3. The methyl hydroperoxide produced can then act as a reservoir in the remote troposphere, producing OH upon photolysis, but is also physically removed by wet deposition.

In the polluted atmosphere where there are high levels of NO_x (NO and NO_2), CH_3O_2 can react with NO to form NO_2 as shown in reaction 4a.[2]

$$CH_3O_2 + NO \rightarrow CH_3O + NO_2 \quad (4a)$$

$$NO_2 + h\nu\ (\lambda < 410\ \text{nm}) \rightarrow NO + O \quad (5)$$

$$O + O_2 + M \rightarrow O_3 + M \quad (6)$$

Ozone is then produced from the photolysis of NO_2 as shown in reactions 5 and 6. Therefore the oxidizing potential and ozone abundance of the troposphere increases. To model the tropospheric abundance of ozone with accuracy, it is necessary to determine the rate coefficient for reaction 4 over the temperature range 200−300 K.

* Corresponding author. E-mail: C.Percival@manchester.ac.uk.
‡ Current address: School of Earth Atmospheric and Environmental Sciences, University of Manchester, The Sackville Street Building, Sackville Street, P.O. Box 88, Manchester, M60 1QD, UK.
† University of Bristol.

10.1021/jp047764b CCC: $27.50
Published on Web 11/09/2004

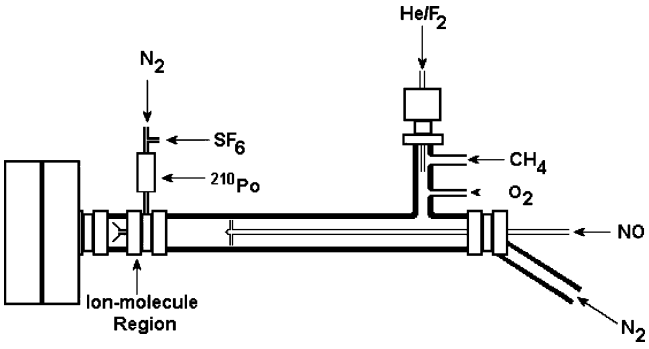

Figure 1. A schematic diagram of the turbulent flow CIMS instrument.

Reaction 4 has been the focus of a considerable number of studies as a consequence of its important role in the formation of tropospheric ozone. In a study by Villalta et al.,[3] experiments were carried out on reaction 4 at temperatures as low as 200 K, and at low total pressures, ~3 Torr. Villalta et al.[3] suggested that at low temperatures and high pressures the association reaction 4b could not be ruled out as a product channel. Although the fraction of methyl nitrate formed in reaction 4b would be small even at atmospheric pressure, its formation could account for the amount of methyl nitrate observed in the troposphere.

$$CH_3O_2 + NO + M \rightarrow CH_3ONO_2 + M \qquad (4b)$$

A more recent study by Scholtens et al.[4] examined the kinetics of reaction 4 but at pressures of 100−200 Torr. At room temperature there was good agreement with the low-pressure study of Villalta et al.,[3] but as the temperature was reduced the two studies diverged, such that at 200 K the high-pressure study yielded a rate coefficient some 50% greater than that determined by the low-pressure study. However, Scholtens et al.[4] were still unable to detect the presence of reaction 4b as a product channel, even though their work suggested that there might be a pressure-dependent component. There is then a possible discrepancy between the two studies or a pressure dependence that is not represented in current evaluations. Hence, the purpose of this paper is to report a kinetic and mechanistic study of reaction 4 performed over an extended temperature range, 193−300 K, and 100−200 Torr to determine whether there is a pressure dependence, to report the first low-temperature evaluation of the branching ratio of reaction 4, and to evaluate the impact of the various low-temperature kinetic studies on tropospheric trace gas composition with use of a chemical box model.

Experimental Section

A schematic diagram of the experimental apparatus is shown in Figure 1. The flow tube was constructed from 22 mm i.d. Pyrex tubing, the walls of which were coated with Halocarbon wax (Halocarbon Products Inc.). A large flow of nitrogen (ranging from 50 to 130 STP L min^{-1}) was injected upstream of the flow tube. The flow tube was pumped by a rotary pump (Varian DS1602). Nitrogen monoxide was injected through a moveable injector constructed from 4 mm i.d. Pyrex. A propeller shaped Teflon piece (a "turbulizer") designed to enhance turbulent mixing was fixed to the end of the moveable injector. All of the experiments were performed under turbulent flow conditions. Turbulent flow is established when the Reynolds number, *Re*, is greater than 3000. This number is given by:

$$Re = \frac{d\bar{u}\rho}{\mu} \qquad (I)$$

where d is the internal diameter of the flow tube, $\bar{u}$ is the average velocity of the carrier gas, μ is the viscosity of the carrier gas, and ρ is the density of the carrier gas.

The ion−molecule region was constructed from 22 mm o.d. Pyrex tubing and a quadrupole mass spectrometer (ABB Extrel Merlin) was located at the end of the flow tube. All gas flows were monitored with calibrated mass flow meters (MKS, 1179). The pressures in the flow tube were monitored with a 0−1000 Torr capacitance manometer (MKS Baratron).

The temperature within the flow tube was maintained within 2 K by placing the flow tube into an insulated chamber that was filled with dry ice. All temperatures were monitored by type K thermocouples. The flow tube temperature was maintained with heating tape (Omega heavy duty) regulated by an electronic controller (Carel Universal Infrared control type W) in conjunction with a thermocouple. The flow tube has 5 thermocouples along its length to monitor the temperature of the system. The nitrogen carrier gas was pre-cooled to the same temperature by passing it through a copper coil immersed in liquid nitrogen. The carrier gas temperature was maintained with heating tape (Omega heavy duty) regulated by an electronic controller (Carel Universal Infrared control type W) in conjunction with a thermocouple. The temperature profile along the flow tube was checked by placing a thermocouple at the end of the moveable injector, and moving it along the length of the flow tube.

CH_3O_2 radicals were produced upstream of the flow tube via the reactions

$$CH_4 + F \rightarrow CH_3 + HF \qquad (7)$$

$$CH_3 + O_2 + M \rightarrow CH_3O_2 + M \qquad (2)$$

Fluorine atoms were produced by combining a 2.0 STP L min^{-1} flow of He with a 0.1 to 3 STP cm^3 min^{-1} flow of 1% F_2 in helium, which was then passed through a microwave discharge produced by a Surfatron cavity (Sairem) operating at 150 W. To produce CH_3 radicals, the F atoms were injected into the flow tube via a sidearm inlet located at the rear of the flow tube and mixed with an excess of CH_4, to ensure that all F atoms were titrated via reaction 1. CH_3O_2 was then produced by the addition of a 1.0 STP L min^{-1} flow of O_2 just downstream from the production of methyl radicals.

NO was introduced into the flow tube via the moveable injector by mixing a flow of 10% NO with a 1 STP L min^{-1} flow of N_2. In all cases, $[NO] \gg [CH_3O_2]$, so that pseudo-first-order conditions were maintained. Blank runs (in the absence of NO) were carried out to ensure that the CH_3O_2 signal (measured at *m/e* 51, i.e., FO_2^-, see later) was not affected by movement of the injector.

NO_2 and CH_3O_2 were chemically ionized with SF_6^- as the reagent ion. SF_6^- was generated by combining a 10 STP L min^{-1} flow of N_2 with a 2.5 STP cm^3 min^{-1} flow of SF_6 and passing it through a ^{210}Po Nuclecel ionizer (NRD Inc.). The generated reagent ion was then carried into the ion−molecule region through an injector constructed from 6 mm o.d. stainless steel tubing. A fan-shaped turbulizer was attached to the end of the inlet to enhance mixing of the reagent ion with the sampled flow from the flow tube. NO_2 was ionized by SF_6^- via electron transfer, enabling detection by the parent ion NO_2^-. CH_3O_2 was detected as FO_2^-, presumably through a multistep pathway. Figure 2 shows the appearance of FO_2^- signal as a function of reactant gases. FO_2^- signal only appears when F atoms, CH_4, and O_2 are present. Also, the FO_2^- signal returns to background levels when CH_4, O_2, or F_2 flows are turned off,

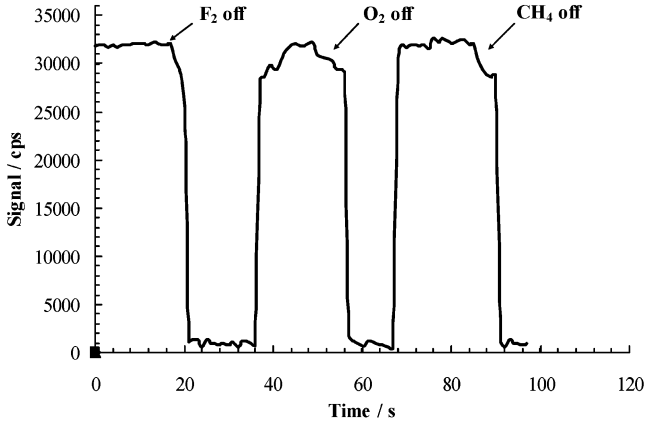

Figure 2. FO_2^- signal production.

thus indicating that FO_2^- can only be attributed to the presence of CH_3O_2 radicals. A simple energetics analysis suggests that the reaction between SF_6^- and FO_2 will produce highly energetic FO_2^- ions and that these then have sufficient energy to decompose to F^- and O_2. Although FO_2 radicals are being formed in the absence of CH_4 they cannot be detected as FO_2^-. We would not like to speculate on the exact mechanism involved in the reaction of SF_6^- with CH_3O_2 to eventually produce FO_2^-, but it would appear that in this case there is insufficient excess energy for them to decompose further.

Ions were detected with a quadrupole mass spectrometer in a three-stage differentially pumped vacuum chamber. A sample of the bulk gas flow containing reactant ions is drawn into the front chamber through a 0.6-mm aperture, which was held at a potential of −70 V to further focus charged reactant molecules. The front vacuum chamber was pumped by a rotary pump (Varian DS402) and held at approximately 2 Torr. The ions were further focused by a 3 cm o.d. and 0.2 mm i.d. stainless steel plate held at −15 V and passed into a second chamber containing the quadrupole mass filter (ABB Extrel, Merlin). This second chamber was pumped by a turbomolecular pump (Varian V250) backed by a rotary pump (Edwards E2M8). The rear chamber that held the multiplier assembly was pumped by a further turbomolecular pump (Varian V250) backed by a rotary pump (Edwards E2M2). Under typical operating conditions the rear chamber was at a pressure of approximately 9×10^{-6} Torr. Ions were detected with a channeltron (Dtech 402A-H) via negative ion counting.

Materials. Helium (BOC, CP Grade) was passed through a gas clean oxygen filter (Chrompak) cartridge to remove traces of oxygen, a Gas clean moisture filter cartridge (Chrompak) to remove H_2O, and a trap held at 77 K containing a molecular sieve (BDH, 4A). NO_2 (98.3%) was purified by repeated freeze−pump−thaw cycles. NO (Technical grade) was purified by freeze−pump−thaw cycles, and selective freezing of NO_2 impurities. N_2, O_2 (99.6%), and CH_4 (99.995%) were used as supplied.

Results and Discussion

Assessment of Detector Sensitivity. Dilute mixtures of NO_2 were injected via the moveable injector into the flow tube with no other gases present and the NO_2^- signal was monitored. From a linear plot of $[NO_2]$ vs NO_2^- signal it is estimated that the sensitivity for NO_2 was 2×10^7 molecule cm^{-3} for a signal-to-noise ratio of 1 and a time constant of 1 s. The NO_2 concentrations were corrected to take into account equilibrium concentrations of N_2O_4 in the gas mixtures used. Under the experimental conditions the lifetime of N_2O_4 formed by the equilibrium

$$NO_2 + NO_2 + M \rightleftharpoons N_2O_4 + M \qquad (8)$$

is comparable with the time of mixing.[5] This assumption was corroborated by the fact that on the time scale of the experiment no change in $[NO_2]$ was observed.

Calibration of the CH_3O_2 signal was achieved by adding a large excess of NO (using a ≥50% NO/He mixture) via the moveable injector at a constant contact time and by monitoring the resultant NO_2 formed by reaction with CH_3O_2

$$CH_3O_2 + NO \rightarrow CH_3O + NO_2 \qquad (4a)$$

Sufficient NO was added to ensure complete removal of CH_3O_2, confirmed by a constant NO_2^- signal with increasing [NO]. It is assumed that $[NO_2]_{observed} = [CH_3O_2]$. This procedure was repeated for several different fluorine atom concentrations and yielded a linear plot of FO_2^- signal vs $[NO_2]_{observed}$. It is estimated that the sensitivity for CH_3O_2 was 1×10^7 molecule cm^{-3} for a signal-to-noise ratio of 1 and a time constant of 1 s. It is interesting to note that at the earth's surface such a sensitivity for CH_3O_2 radicals corresponds to a volume mixing ratio of ∼0.5 ppt (parts per trillion). Measurements of peroxy radicals in the atmosphere have been made by using the PERCA (Peroxy Radical Chemical Amplification) technique,[6] which converts all peroxy radicals to alkoxy radicals by reaction with NO and monitors the NO_2 produced. Typical "total" or sum of peroxy radical values measured by this technique in the troposphere is in the low ppt range. Another technique, Matrix Isolation Electron Spin Resonance (MIESR),[7] can also measure total organic peroxy radicals, but is capable of providing speciated peroxy radical levels. PERCA can make measurements on the second time scale, whereas MIESR requires many minutes to collect sufficient sample for a measurement to be made. Ideally, one would want second to minute time resolution offered by PERCA, but have speciated peroxy radical measurements offered by MIESR. Recently Hanke et al.[8] have utilized the sensitivity of the CIMS technique to develop a chemical conversion/CIMS technique, ROXMAS. This is essentially an extension of the PERCA technique whereby peroxy radicals are converted to sulfuric acid via a chain reaction. The technique enables peroxy radicals to be measured with a 1 min time resolution with an absolute sensitivity of 0.5 ppt (v). While the ROXMAS technique represents a significant enhancement in sensitivity it does not directly detect the parent ions of the radical species and consequently cannot provide direct information on the speciation of peroxy radicals in the atmosphere. The potential of SF_6^- ion chemistry for the detection of atmospheric data has already been demonstrated.[9] Therefore, the CIMS technique utilizing SF_6^- as a precursor ion would appear to be an exciting potential field instrument, having the necessary sensitivity, sampling rate, and selectivity. Clearly, further laboratory development is required, but there is already the inherent sensitivity to make measurements of these extremely important radicals in the atmosphere.[10]

Rate Coefficient Determination. The rate coefficient for reaction 4 was measured by monitoring CH_3O_2 concentration profiles at *m/e* 51 under pseudo-first-order conditions with $[CH_3O_2] = (1-10) \times 10^{10}$ molecule cm^{-3} and $[NO] = (1-13) \times 10^{12}$ molecule cm^{-3}. First-order decay rates (k_{1st}) were obtained by a linear regression of the plots of ln(CH_3O_2 signal) vs contact time (as shown in Figure 3). Contact times were

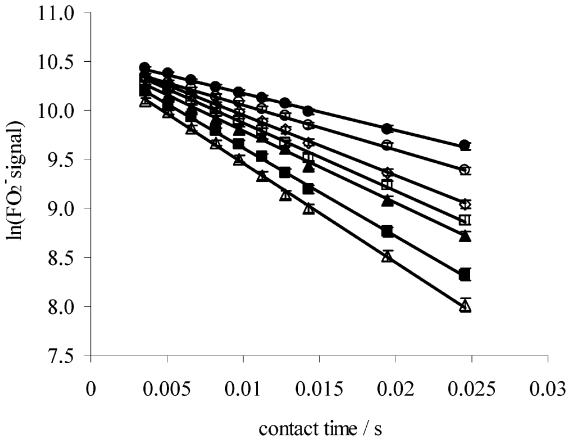

Figure 3. A typical set of pseudo-first-order plots for [NO] of (●) 2.88×10^{12}, (○) 4.32×10^{12}, (◇) 5.76×10^{12}, (□) 7.20×10^{12}, (▲) 8.64×10^{12}, (■) 1.01×10^{13},[3] and (△) 1.15×10^{13} molecules cm^{-3}.

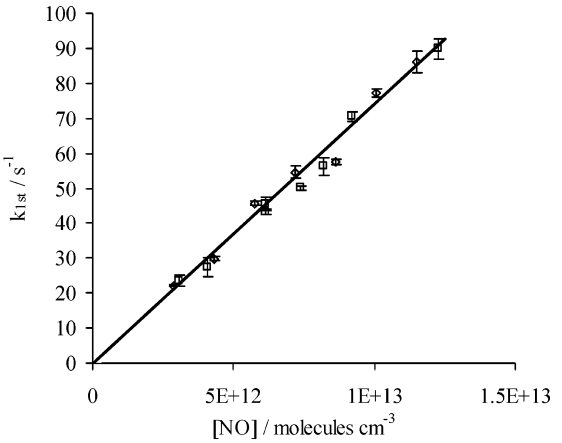

Figure 4. Second-order plot showing the results of experiments at two different pressures at 300 K: (◇) 200 and (□) 100 Torr data. The line is the linear least-squares fit.

determined by dividing the injector−detector distance by the average gas velocity. These plots were essentially linear for all the experiments, indicating the absence of any secondary chemistry effects. This process was repeated for at least ten different values of [NO] at each pressure studied. The values of k_{1st} were then plotted vs [NO] as shown in Figure 4. These data points were fitted with a linear least-squares routine, the slope of which provided the effective bimolecular rate constant, k_4. This approach for the determination of the effective bimolecular rate coefficient assumes that deviations from the plug flow approximation are negligible. Under the experimental conditions used, Seeley et al.[11] estimated that deviations from the plug flow approximation result in apparent rate coefficients that are at most 8% below the actual values. Other workers,[12,13] using different flow system configurations, have found the need to apply small corrections to the plug flow approximation in order to obtain accurate results when using the turbulent flow technique as a result of small deviations from the ideal conditions described by Seeley et al.[11] However, since no systematic errors[11,14] have been apparent in the systems that have been studied to date with the present flow configuration, no correction to the plug flow approximation is applied here.

The data shown in Figure 4 are for experiments carried out at two different pressures at 298 K. Within error each data set produces the same effective bimolecular rate coefficient indicating that the rate coefficient is invariant with pressure. If all these data are combined an effective bimolecular rate coefficient at

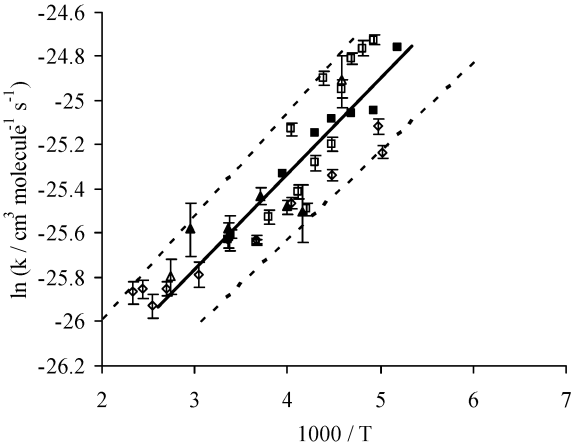

Figure 5. Arrhenius plot for the CH_3O_2 + NO reaction. The solid line is the linear least-squares fit to data points from this work. The dashed line is equivalent to one standard deviation. Data from (■) this work, (□) Scholtens et al.,[4] (△) Simonaitis and Heicklen,[17] (◇) Villalta et al.,[3] and (▲) Ravishankara et al.[18] For clarity error bars have only been included that are larger than the size of the symbols.

TABLE 1: Experimentally Determined Rate Constants for the Reaction CH_3O_2 + NO

temp, K	velocity, cm s^{-1}	R_e	pressure, Torr	rate coefficient, $\times 10^{-12}$ cm^3 $molecule^{-1}$ s^{-1}
298	1750	3238	100	7.41 ± 0.22
298	962	3561	200	7.42 ± 0.17
253	1624	4065	100	9.97 ± 0.10
233	747	4341	200	12.01 ± 0.04
223	1431	4499	100	12.82 ± 0.08
213	870	5945	200	13.09 ± 0.08
203	1302	4860	100	13.25 ± 0.07
193	788	6453	200	17.67 ± 0.16

298 K of $(7.42 \pm 0.27) \times 10^{-12}$ cm^3 $molecule^{-1}$ s^{-1} is obtained, which is in excellent agreement with previous studies.[3,4,15−18]

The rate coefficient for reaction 4 was also studied over the temperature range 193−300 K. Table 1 summarizes the effective bimolecular rate coefficients obtained in this study. The uncertainty associated with the rate coefficients is given at the one standard deviation level from a 95% confidence limit linear least squares routine fit of the second order plot. The rate coefficients increased by approximately 40% as the temperature was lowered from 300 to 193 K. The rate coefficients were determined as a function of pressure from 100 to 200 Torr, and no effect of pressure on the measured rate coefficients was observed over the temperature range studied. Using the data in Table 1 it is possible to carry out an Arrhenius type analysis of the temperature dependence yielding an "Arrhenius" expression of $k(T) = (1.75^{+0.28}_{-0.24}) \times 10^{-12} \exp[(435 \pm 35)/T]$ cm^3 $molecule^{-1}$ s^{-1}, i.e., an apparent negative activation energy is observed. The uncertainty associated with the rate coefficients is given at the one standard deviation level.

Comparison with Previous Studies. Four other studies have been carried out to investigate the temperature dependence of the rate coefficient for reaction 4 below 300 K. Three studies were carried out at pressures ≥100 Torr: a high-pressure flow tube study by Scholtens et al.[4] and two flash photolysis studies at a few selected temperatures (365, 296, and 218 K) by Simonaitis and Heicklen[17] and Ravishankara et al.[18] (339, 298, 270, 250, and 240 K). There has also been the low-pressure flow tube study of reaction 4 by Villalta et al.[3] A comparison of data from this study with previous low-temperature studies is shown in Figure 5. The results of Ravishankara et al.,[18] reveal a very small temperature dependence, in fact these workers

report that the reaction is temperature independent, which is in disagreement with all other temperature studies of reaction 4. Ravishankara et al.[18] monitored the formation and decay of NO_2 in their flash photolysis system and used this to determine the concentration of CH_3O_2 in their experiment. Their analysis required careful corrections for quantities such as laser fluence and it is possible that the lack of an observed temperature dependence stems from this conversion. It is interesting to note that at 298 K, where they made measurements at three pressures (40, 50, and 100 Torr), their reported rate coefficient decreases from 8.0×10^{-12} to 7.5×10^{-12} cm^3 molecule^{-1} s^{-1} as pressure is increased from 40 to 100 Torr, but is effectively pressure independent as all three measurements are within the combined experimental error. The work of Simonaitis and Heicklen[17] consists of one subambient rate coefficient determination that is in broad agreement with the study of Scholtens et al.[4] Therefore we will restrict our discussion to the two most recent studies. Essentially, Figure 5 shows that the low-temperature rate coefficients determined in this study lie between the studies of Scholtens et al.[4] (high pressure) and Villalta et al.[3] (low pressure). Is the difference between the two previous studies evidence for a pressure-dependent channel?

Does k_4 Have a Pressure-Dependent Channel? The negative temperature dependence of the rate coefficient for reaction 4 suggests that it proceeds through the formation of an [CH_3-OONO]* intermediate. The intermediate could then re-dissociate back to reactants, undergo bond fission to yield products, isomerize to form methyl nitrate, or undergo collisional stabilization. The elements of the mechanism may be summarized as:

$$CH_3O_2 + NO \rightarrow [CH_3OONO]^* \quad (9)$$

$$[CH_3OONO]^* \rightarrow CH_3O_2 + NO \quad (-9)$$

$$[CH_3OONO]^* \rightarrow CH_3O + NO_2 \quad (10)$$

$$[CH_3OONO]^* + M \rightarrow CH_3OONO + M \quad (11)$$

$$[CH_3OONO]^* + M \rightarrow CH_3ONO_2 + M \quad (12)$$

A pressure-dependent channel is likely to be favored by low temperatures. First it is worth noting that at 203 K (lowest temperature reported by all three studies) the three studies report the following rate coefficients: $(18.3 \pm 4.0) \times 10^{-12}$ cm^3 molecule^{-1} s^{-1} at 100 Torr,[4] $(13.25 \pm 0.73) \times 10^{-12}$ cm^3 molecule^{-1} s^{-1} at 100 Torr (this work), $(12.30 \pm 0.38) \times 10^{-12}$ cm^3 molecule^{-1} s^{-1} at 4.8 Torr,[3] and $(12.40 \pm 0.49) \times 10^{-12}$ cm^3 molecule^{-1} s^{-1} at 1.95 Torr (at 200 K).[3] There is no significant difference between the rate coefficients determined by us and Villalta and co-workers[3] within experimental error and hence no pressure-dependent channel can be inferred. Second, inspection of the kinetic measurements by Villalta et al.[3] at different pressures but at the same temperature (223 and 248 K) shows agreement within error, and shows if anything a decrease in rate coefficient with increasing pressure. We would conclude that although the rate coefficients measured in this study are consistently higher than those of Villalta et al.,[3] within the combined error there is no difference between the two studies. This study does not support the findings of Scholtens et al.,[4] that at pressures of 100−200 Torr and T < 220 K, k_4 is some 50% higher than the rate coefficient determined by Villalta et al.[3] at pressures of 1−5 Torr. There is no obvious reason the measurements of Scholtens and co-workers should be much higher than ours at low temperature, and we cannot offer a sensible explanation, although it should be noted that the errors associated with working at low temperature increase considerably.

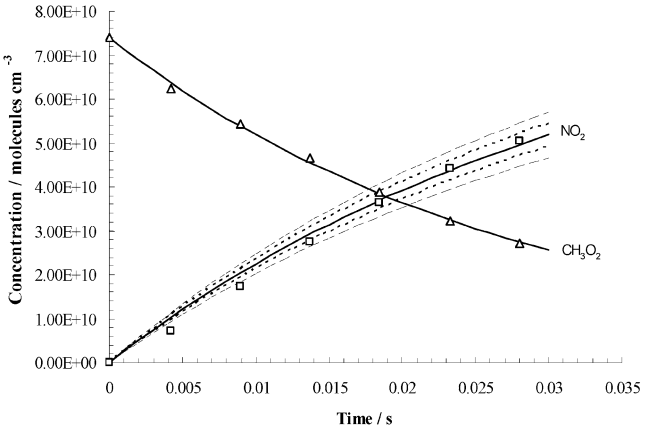

Figure 6. Signal intensity as a function of injector position: (△) CH_3O_2 and (□) NO_2. The solid line represents $\alpha = 1$, the dotted line represents $\alpha = 0.95$, and the dashed line represents $\alpha = 0.9$.

Recently, Lohr et al.[19] and Barker et al.[20] have carried out very detailed theoretical calculations to determine the alkyl nitrate yields from the general reaction of peroxy radicals with NO. In these studies they used G3 and B3LYP/6-311++G** levels of theory to determine the geometries, energies, and vibrational frequencies for major stationary points on the potential energy surfaces and then Master Equation calculations to determine branching ratios. One of the systems studied was reaction 4, where it would appear that no pressure dependence is expected, since the initial CH_3OONO intermediate rapidly decomposes to yield CH_3O and NO_2, i.e. reaction 10 is much faster than reaction −9, 11, or 12. This work would support this assertion.

Branching Ratio Evaluation. Attempts were made to assess the branching ratio of reaction 4, via the direct detection of CH_3-ONO_2. CH_3ONO_2 was synthesized via the nitration of methanol,[4] unfortunately with the ionization scheme used, CH_3ONO_2 could not be detected. The branching ratio of reaction 4 was measured indirectly via the measurement of [CH_3O_2] and [NO_2] as a function of contact time, as shown in Figure 6. The concentration−time profiles of CH_3O_2 and NO_2 were modelled by using the kinetic model given in Table 3. Each reaction rate constant in the used kinetic model was altered individually by an order of magnitude the affect on the predicted growth decay curves assessed. No effect on NO_2 production was observed with the notable exception of HO_2 + NO. However, within experimental errors quoted by Bardwell et al.,[21] or the experimental errors suggested by Sander et al.,[22] no appreciable affect on the NO_2 concentration time profiles was observed. The modelled fits were obtained assuming 100% formation of NO_2, i.e., a branching ratio of 1. Over the temperature and pressure range studied there was no evidence, within experimental error, for the formation of any stabilized adducts or secondary product channels, i.e., it can be assumed that the reaction proceeds 100 ± 10% via the formation of CH_3O and NO_2, where the quoted error reflects the range of branching ratios for reaction 4 that could be used to model these data satisfactorily. Figure 6 illustrates the sensitivity of the modelled NO_2 concentration time profiles to the value of the branching ratio of reaction 4. The inner dashed lines represent a confidence level of ±5% and the outer dashed lines ±10%.

There have been three room temperature evaluations of the branching ratio of reaction 4[4,15,23] and a comparison with the

TABLE 2: A Comparison of Arrhenius Parameters for the Reaction of CH_3O_2 + NO

Study	temp, K	pressure, Torr	$-E_a/R$, kJ mol^{-1}	A factor, $\times 10^{-12}$ cm^3 molecule^{-1} s^{-1}
Ravishankara et al.[18]	240−339	100	86 ± 112	6.3 ± 2.5
Scholtens et al.[4]		100−200	600 ± 140	$0.93^{+0.06}_{-0.04}$
Simonaitis and Heicklen[17]	218−365	100−600	380 ± 250	2.1 ±1.0
Villalta et al.[3]	199−429	2−5	285 ± 65	2.8
this work	193−298	100−200	435 ± 35	$1.75^{+0.28}_{-0.24}$

TABLE 3: A Summary of the Chemical Reactions Used To Asses the Branching Ratio for the Reaction of CH_3O_2 + NO

reaction	A/cm^3 s^{-1} molecule^{-1}	$E/R_{\pm}$ ($\Delta E/R$)	k(298 K)‡
$CH_3O_2 + NO \rightarrow CH_3O + NO_2$	1.8×10^{-12}	−(435 ± 35)	7.70×10^{-12}
$CH_3O_2 + CH_3O_2 \rightarrow 2\ CH_3O + NO$	$2.5 \times 10^{-13-}$	-(190 ± 190)	4.70×10^{-13}
$CH_3O + O_2 \rightarrow CH_2O + HO_2$	3.9×10^{-14}	(900 ± 300)	1.90×10^{-15}
$HO_2 + NO \rightarrow NO_2 + OH$	3.5×10^{-12}	−(250 ± 50)	8.10×10^{-12}
$OH + HO_2 \rightarrow H_2O + O_2$	4.8×10^{-11}	−(250 ± 200)	1.10×10^{-10}
$OH + OH \rightarrow H_2O + O$	4.2×10^{-12}	(240 ± 240)	1.90×10^{-12}
$OH + CH_2O \rightarrow H_2O + CO$	8.2×10^{-12}	(333 ± 12)	9.40×10^{-12}

	k_0^{300}/cm^6 s^{-1} molecule^{-2}		k_∞^{300}/cm^3 s^{-1} molecule^{-1}		
reaction	k_0^{300}	M	k_∞^{300}	n	k(298 K)
$OH + OH \rightarrow H_2O_2$	6.2×10^{-31}	1	2.6×10^{-11}	0	1.49×10^{-12}
$OH + NO \rightarrow HONO$	7.0×10^{-31}	2.6	3.6×10^{-11}	0.1	1.82×10^{-12}
$OH + NO_2 \rightarrow HNO_3$	2.5×10^{-30}	4.4	1.6×10^{-11}	1.7	3.43×10^{-12}
$CH_3O_2 + NO_2 \rightarrow CH_3O_2NO_2$	1.5×10^{-30}	4.0	6.5×10^{-12}	2.0	1.72×10^{-12}
$CH_3O + NO \rightarrow CH_3ONO$	1.4×10^{-29}	3.8	3.6×10^{-11}	0.6	1.23×10^{-11}
$CH_3O + NO_2 \rightarrow CH_3ONO_2$	1.1×10^{-28}	4.0	1.6×10^{-11}	1.0	1.29×10^{-12}

(k_{298K} in cm^3 molecule^{-1} s^{-1}) taken from Sander *et al.*[22]

TABLE 4: A Comparison of Branching Ratios at 298 K for the Reaction of CH_3O_2 + NO To Form CH_3O + NO_2

study	branching ratio $k_{4a}/(k_{4a} + k_{4b})$
Ravishankara et al.[18]	>0.76
Zellner et al.[23]	>0.8
Scholtens et al.[4]	>0.97
this work	1.0 ± 0.1

results of this study is given in Table 4. All three studies are in agreement with this work suggesting that there is little or no experimental evidence for the formation of CH_3ONO_2. Lohr et al.[19] and Barker et al.[20] conclude that the barrier to isomerization from CH_3OONO to CH_3ONO_2 is high (∼136 kJ mol^{-1}) compared with the barrier for simple bond fission from CH_3-$OONO$ to CH_3O and NO_2 (∼50 kJ mol^{-1}). Although Ellison et al.[24] find a lower barrier to isomerization (80−120 kJ mol^{-1}) the conclusion from these theoretical studies is that the yield of methyl nitrate from this reaction is negligible. With this in mind one would not expect the branching ratio to increase with decreasing temperature, a fact that is totally consistent with this study. The errors associated with the reported branching ratios in this study are relatively large, being based on NO_2 production. Further work is required to monitor the methyl nitrate directly as a function of temperature, to reduce further the errors in the branching ratio.

Atmospheric Implications. The importance of reaction 4 for the in situ production of ozone in the troposphere is well-known.[25] We have therefore carried out two sensitivity studies using a box model: In the first we have assessed the impact of the errors associated with the rate coefficients determined in this study on the main tropospheric species including O_3, NO, NO_2, OH, and HO_2. In the second we have assessed the impact on these and other species by running the model using each of the Arrhenius parameters given by the four previous studies carried out at subambient temperatures and this work. Model sensitivity studies have been performed, using CiTTy CAT, a tropospheric trajectory model.[26] The model was run for a variety of scenarios, replicating those conditions prescribed in the Photochemistry-Intercomparison Exercise.[27] Details of the initial conditions and model scenarios used can be found in the summary paper by Olson et al.[27] Essentially, the model was run under three surface scenarios, clean marine, background continental, and urban conditions, and two scenarios away from the surface, a polluted plume at 4 km and a clean air scenario at 8 km. These five scenarios were originally chosen for the intercomparison to cover the range NO_x/VOC encountered in the troposphere and its influence on ozone production and destruction. The CiTTy CAT model contains a detailed chemistry scheme with 13 non-methane hydrocarbons and for each scenario the model was integrated forward in box model mode for 5 days. For the first experiment, three integrations were performed for each of the five atmospheric conditions described: a base case where the central Arrhenius parameters derived in this study were used, a "high" k_4 case, where the largest A factor and lowest E_a, within measurement error in this study were used, and a "low" k_4 case, where the smallest A factor and highest E_a, within measurement error in this study, were used. In all cases, within the experimental error of this study, model O_3 did not deviate by more than 0.5%. The model OH concentration varies by 1−2% over the entire range of NO_x and HO_2 likewise varies rather modestly (1−3%), irrespective of altitude. NO and NO_2 vary by a few percent over the entire range of scenarios. Only methyl peroxy radicals (12% at 8 km) vary significantly, where an increase in the rate constant reduces the model concentration and vice versa. It is concluded that the impact of the experimental error in the measurement of k_4 in this study has an insignificant effect on modelled species concentrations in the troposphere.

For the second experiment, the central values for each set of Arrhenius parameters from the five studies were used. Once again there is no significant impact on O_3 in the model; however, there is a spread in model concentrations for the species CH_3O_2 (25%), HCHO (11%), HO_2NO_2 (7%), $CH_3O_2NO_2$ (20%), and HO_2 (3%) at 8 km (T = 236 K). It should be noted that adopting

the higher value for k_4 increases the yield of HO_2NO_2 and HCHO while decreasing the yield of CH_3O_2 and $CH_3O_2NO_2$ and vice versa. Therefore, subtle changes to k_4 drive the partitioning between HO_2NO_2 and $CH_3O_2NO_2$ apart. Such deviations may have important implications for observationally driven models of the upper troposphere, where the fluxes of reservoirs such as HO_2NO_2 and $CH_3O_2NO_2$ are poorly constrained.[25] Further integrations at 8 km but adopting a lower temperature increase the discrepancy still further, as expected, such that at 200 K the difference between high and low values of the rate coefficient for HO_2NO_2 is 14% and $CH_3O_2NO_2$ is approaching 30%. Finally, the model is very sensitive to the rate of formation of HO_2NO_2 and $CH_3O_2NO_2$, and therefore the rate coefficients for reactions 13 and 14 warrant study at low temperatures and over a range of pressure.

$$HO_2 + NO_2 + M \rightarrow HO_2NO_2 + M \quad (13)$$

$$CH_3O_2 + NO_2 + M \rightarrow CH_3O_2NO_2 + M \quad (14)$$

Conclusions

Our data indicate that reaction 4 has a significant negative temperature dependence, as suggested by previous studies of the reaction.[3,4,17] The results presented in this article represent an extension in the range of temperatures over which reaction 4 has been studied experimentally. The negative temperature dependence of the rate coefficient for reaction 4 suggests that it proceeds through the formation of an energized intermediate (CH_3OONO^*). Over the temperature range studied the rate coefficient for reaction 4 was found to be invariant with pressure and does not support the assertion by Scholtens and co-workers[4] that at low temperatures high- and low-pressure measurements differ by 50%. In conjunction with product studies and theoretical calculations,[19,20] our results suggest that the CH_3OONO^* intermediate is too short-lived to be affected by collisions and it exclusively decomposes via simple bond fission to yield CH_3O and NO_2. Sensitivity studies, using a tropospheric trajectory model, were performed to assess the impact of the experimental errors associated with k_4 from this study on tropospheric O_3 production. It was found that within the experimental error of the studies, model O_3 did not deviate by more than 1%. However, if one uses the Arrhenius parameters derived from previous studies, at low temperatures typical of the upper troposphere, significant differences arise for the model concentrations of CH_3O_2, HCHO, HO_2NO_2, and $CH_3O_2NO_2$. Such a finding may be important for observationally driven models applied to the upper troposphere.[28]

Acknowledgment. The authors gratefully acknowledge the financial support of NERC research grant reference no. NER/T/S/1999/00111. M.B. thanks NERC for a studentship and G.S.-R. thanks the Instituto Mexicano del Petróleo for a studentship. The Biogeochemistry research centre at Bristol is a joint initiative between the School of Chemistry and the Departments of Geography and Earth Sciences.

References and Notes

(1) Wayne, R. P. *Chemistry of Atmospheres*, 3rd ed.; Oxford University Press: Oxford, UK, 2000.
(2) Finlayson-Pitts, B. J.; Pitts, J. N., Jr. *Atmospheric Chemistry*; John Wiley and Sons: New York, 1986.
(3) Villalta, P. W.; Huey L. G.; Howard, C. J. *J. Phys. Chem.* **1995**, *99*, 12829−12834.
(4) Scholtens, K. W.; Messer, B. M.; Cappa C. D.; Elrod, M. J. *J. Phys. Chem.* **1999**, *103*, 4378−4384.
(5) Borrell, P.; Cobos, C. J.; Luther, K. *J. Phys. Chem.* **1988**, *92*, 4377−4384.
(6) Cantrell, C. A.; Stedman, D. H.; Wendel, G. J. *Anal. Chem.* **1984**, *56*, 1496−1502.
(7) Mihelcic, D.; Klemp, D.; Musgen, P.; Patz, H. W.; Volz-Thomas, A. *J. Phys. Chem.* **1993**, *16*, 313−335.
(8) Hanke, M.; Uecker, J.; Reiner, T.; Arnold, F. *Int. J. Mass. Spectrum.* **2002**, *213*, 91−99.
(9) Slusher, D. L.; Pitteris, S. J.; Haman, B. J.; Tanner, D. J.; Huey, L. G. *Geophys. Res. Lett.* **2001**, *28*, 3875−3878.
(10) Clemitshaw, K. C. *Crit. Rev. Environ. Sci. Technol.* **2004**, *34*, 1−108.
(11) Seeley, J. V.; Jayne, J. T.; Molina, M. J. *Int. J. Chem. Kinet.* **1993**, *25*, 571−594.
(12) Chuong, B.; Stevens, P. S. *J. Geophys. Res.* **2002**, *107*, 4162−4173.
(13) Herndon, S. C.; Villalta, P. W.; Nelson, D. D.; Jayne, J. T.; Zahniser, M. S. *J. Phys. Chem. A* **2001**, *105*, 1583−1591.
(14) Miller, A. A.; Yeung, L. Y.; Kiep, A. C.; Elrod, M. *J. Phys. Chem. Chem. Phys.* **2004**, *6*, 3402−3407.
(15) Sehested, J.; Nielsen, O. J.; Wallington, T. J. *Chem. Phys. Lett.* **1993**, *213*, 454−467.
(16) Lightfoot, P. D.; Cox, R. A.; Crowley, J. N.; Destriau, M.; Hayman, G. D.; Jenkin, M. E.; Moortgat, G. K.; Zabel, F. *Atmos. Environ.* **1992**, *26*, 1805−1961.
(17) Simonaitis, R.; Heicklen, J. *J. Phys. Chem.* **1981**, *85*, 2946−2949.
(18) Ravishankara, A. R.; Eisele, F. L.; Kreutter, N. M.; Wine, P. H. *J. Chem. Phys.* **1981**, *74*, 2267−2274.
(19) Lohr, L. L.; Barker, J. R.; Shroll, R. M. *J. Phys. Chem. A* **2003**, *107*, 7429−7433.
(20) Barker, J. R.; Lohr, L. L.; Shroll, R. M.; Reading, S. *J. Phys. Chem. A* **2003**, *107*, 7434−7444.
(21) Bardwell, M. W.; Bacak, A.; Raventos, M. T.; Percival, C. J.; Sanchez-Reyna, G.; Shallcross, D. E. *Phys. Chem. Chem. Phys.* **2003**, *5*, 2381−2385.
(22) Sander, S. P.; Friedl, R. R.; Ravishankara, A. R.; Golden, D. M.; Kolb, C. E.; Kurylo, M. J.; Huie, R. E.; Orkin, V. L.; Molina, L. T.; Moortgat, G. K.; Finlayson-Pitts, B. J. *Chemical Kinetics and Photochemical Data for Use in Atmospheric Studies*; The Jet Propulsion Laboratory, 2003; Evaluation No. 14, JPL 02-25, web reference: http://jpldataeval.jpl.nasa.gov
(23) Zellner, R.; Fritz, B.; Lorenz, K. *J. Atmos. Chem.* **1986**, *4*, 241−251.
(24) Ellison, G. B.; Blanksby, S. J.; Jochnowitz, E. B.; Stanton, J. F. Manuscript in preparation.
(25) Roelofs, G. J.; Lelieveld, J. *Tellus* **1997**, *49B*, 38−55.
(26) Evans, M. J.; Shallcross, D. E.; Law, K. S.; Wild, J. O. F.; Simmonds, P. G.; Spain, T. G.; Berrisford, P.; Methven, J. V.; Lewis, A. C.; McQuaid, J. B.; Pilling, M. J.; Bandy, B. J.; Penkett, S. A.; Pyle, J. A. *Atmos. Environ.* **2000**, *34*, 3843−3863.
(27) Olson, J.; Prather, M.; Bernsten, T.; Carmichael, G.; Chatfield, R.; Connell, P.; Derwent, R.; Horrowitz, L.; Jin, S.; Kanakidou, M.; Kasibhatla, P.; Kotamarthi, R.; Kuhn, M.; Law, K.; Penner, J.; Perliski, L.; Sillman, S.; Stordal, F.; Thompson, A.; Wild, O. *J. Geophys. Res.* **1997**, *102*, 5979−5991.
(28) Murphy, J. G.; Thornton, J. A.; Wooldridge, P. J.; Day, D. A.; Rosen, R. S.; Cantrell, C. A.; Shetter, R. E.; Lefer, B.; Cohen, R. C. *Atm. Chem. Phys.* **2004**, *4*, 377−384.